Zintl Anions as Starting Compounds for the Synthesis of Polynuclear Transition Metal Complexes

Reinhart Ahlrichs, Dieter Fenske,* Katharina Fromm, Harald Krautscheid, Ulrike Krautscheid, and Oliver Treutler

Dedicated to Professor Kurt Dehnicke on the occasion of his 65th birthday

Abstract: The Zintl anion P_7^{3-} reacts with complexes of transition metal halides to form multinuclear metal phosphorus clusters. Reaction of $Li_3P_7 \cdot 3DME$ with $[FeCp(CO)_2Br]$ or $[NiCl_2(PBu_3)_2]$ leads to the formation of $[P_7\{FeCp(CO)_2\}_3]$ (**1**) and $[\{Ni(PBu_3)_2\}_4P_{14}]$ (**2**), respectively. X-ray structure determinations show that in **1** the P_7 cage of Li_3P_7 remains intact, but in **2** a P_{14} framework is formed by linkage of two norbornadiene-like P_7 units. The P_{14} skeleton coordinates to four $Ni(PBu_3)_2$ groups. LiCp* and $CoCl_2$ react with $P_7(SiMe_3)_3$ to give $[(Cp^*Co)_3(P_2)_3]$ (**3**) with three Cp*Co groups bridged by P_2 units. Reaction of $FeCl_2$ and LiCp* with $P_7(SiMe_3)_3$ yields $[(Cp^*Fe)_3P_6][FeCl_3(thf)]$ (**4**) or $[(Cp^*Fe)_3\{(\eta^3\text{-}P_3)Fe\}P_6]$ (**5**), depending on the reaction conditions. In **4** the structure of the Fe_3P_6 core of the $[(Cp^*Fe)_3P_6]^+$ cation is comparable to *closo*-$B_9H_9^{2-}$, while in **5** the Fe_4P_6 core does not obey the Wade rules. The unusual Co–As cluster $[Co_6As_{12}(PEt_2Ph)_6]$ (**6**), prepared from K, As, and $[CoCl_2(PEt_2Ph)_2]$, can be described as a Co_6As_6 heteroicosahedron linked to two Co_3As_3 octahedra by common Co_3 faces. A theoretical treatment within the density functional approximation reproduces the experimental structures of **2** and **6** and allows an interpretation of molecular electronic structures. In **2** one finds P–P double bonds that are delocalized to some extent into vacant Ni AOs. For the cage compound **6** the Co 3d AOs participate in cage bonding and 38 electrons can be assigned to cage bonds; this is in accord with the $(2N + 2)$ rule for 18-atom cages but not with the usual electron counting rules.

Keywords
crystal structure · density functional calculations · polyarsenido complexes · polyphosphido complexes · Zintl anions

Introduction

Molecular and ionic compounds containing Group 15 elements have been the subject of intense investigation over a long period of time. In particular the variety of structures in polyphosphorus derivatives is impressive, which is shown by the work of Baudler et al. and von Schnering et al.[1] However, there are only a few examples of the reaction of these compounds as ligands for transition metal complexes. Investigations of Fritz et al. showed that $Li_3P_7 \cdot 3DME$ reacts with $[FeCp(CO)_2Br]$ to form $[P_7\{FeCp(CO)_2\}_3]$ (**1**); the structure was determined by ^{31}P NMR spectroscopy, but no crystal structure was available.[2] Baudler et al. reported the formation of $[(\eta^5\text{-}P_5)Mn(CO)_3]$ by reaction of $[Mn(CO)_5Br]$ with LiP_5.[3] There are a large number of complexes with P_n and As_n ligands known, which were synthesized by Scherer and Scheer by reaction of white phosphorus or arsenic with transition metal complexes.[4, 5, 6] Recently Eichhorn et al. reported the reaction of metal(0) complexes with Rb_3As_7 or K_3E_7 (E = P, As, Sb)[7, 8, 9] from which anionic species like $[As_7Cr(CO)_3]^{3-}$ and $[Sb_7Ni_3(CO)_3]^{3-}$ were isolated. Reaction of Rb and As in an Nb ampule gives $^1_\infty[Rb\{NbAs_8\}]^{2-}$ containing Zintl anions.[10]

Except for the syntheses of $[(\eta^5\text{-}P_5)Mn(CO)_3]$ and $[P_7\{FeCp(CO)_2\}_3]$, no further reactions of metalated or silylated polyphosphides with transition metal complexes have been reported. The driving force of this type of reaction is the formation of metal salts or trimethylsilyl halides. For several years this principle has been utilized for reactions of phosphine complexes of transition metal halides with $E(SiMe_3)_2$ (E = S, Se, Te) or $E'(SiMe_3)_3$ (E' = P, As, Sb). A large number of transition metal clusters containing S, Se, Te, P, As, or Sb as bridging ligands have been isolated.[11]

Results and Discussion

In continuation of the work described in the introduction, the reactions of $Li_3P_7 \cdot 3DME$, $P_7(SiMe_3)_3$, or "K_3As_7" (prepared in liquid NH_3, K:As = 3:7) with transition metal complexes are now under investigation. $Li_3P_7 \cdot 3DME$ reacted with $[FeCp(CO)_2Br]$ to form $[P_7\{FeCp(CO)_2\}_3]$ (**1**)[12] [Eq. (a)]. This trans-

$$Li_3P_7 \cdot 3DME + 3[FeCp(CO)_2Br] \longrightarrow \underset{\mathbf{1}}{[P_7\{FeCp(CO)_2\}_3]} + 3LiBr \quad (a)$$

[*] Prof. Dr. D. Fenske, Dr. K. Fromm, Dr. H. Krautscheid, Dipl.-Chem. U. Krautscheid
Institut für Anorganische Chemie der Universität
Engesserstrasse, Geb. 30.45, D-76128 Karlsruhe
Telefax: Int. code +(721)661 921
Prof. Dr. R. Ahlrichs, Dipl.-Chem. O. Treutler
Institut für Physikalische Chemie der Universität Karlsruhe
Kaiserstrasse 12, D-76128 Karlsruhe

0947-6539/96/0202-0238 $ 10.00+.25/0

formation was also reported by Fritz et al,[2] and **1** was described as an unstable compound that decomposes in vacuo. The ^{31}P NMR spectrum of the red needles of **1** is identical with literature data.[2]

Figure 1 shows the P_7 nortricyclane frame of **1**. The [FeCp(CO)$_2$] groups are coordinated by the P atoms P4, P5, and P6, which have two bonds to other P atoms and carry a negative charge according to the Zintl–Klemm concept. The P–P bond lengths of the basal triangle P1, P2, and P3 are 220.3–220.9(3) pm. The distances to the equatorial P atoms are similar: P1–P4 221.1(2); P2–P5 220.2(2); P3–P6 220.0(2) pm. The bond lengths to the apical P atom, P7, are slightly shorter (217.9–218.6(3) pm). These bond parameters correspond with those found in P_7R_3 (R = $SiMe_3$, $SiPh_3$).[2, 13] This shows that the SiR_3 and the [FeCp(CO)$_2$] substituents have a similar influence on the bonding in the P_7 cage.

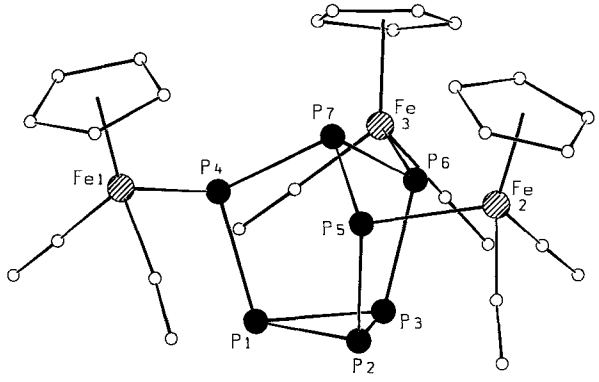

Fig. 1. Molecular structure of **1**. Selected distances [±0.2 pm] and angles [±0.1°]: P1–P2 220.6, P2–P3 220.9, P1–P3 220.3, P1–P4 221.1, P2–P5 220.2, P3–P6 220.0, P4–P7 218.0, P5–P7 218.6, P6–P7 217.9, Fe1–P4 232.8, Fe2–P5 232.5, Fe3–P6 232.8, P2-P1-P3 60.14, P1-P2-P3 59.84, P1-P3-P2 60.02, P1-P4-P7 100.83, P2-P5-P7 100.92, P3-P6-P7 100.69, P4-P7-P6 99.66, P4-P7-P5 98.83, P5-P7-P6 100.32.

Reaction of [$NiCl_2(PR_3)_2$] (R = Et, Pr, Bu, Ph) with $Li_3P_7 \cdot 3\,DME$ or $P_7(SiMe_3)_3$ led to the formation of dark brown solutions, but so far crystals have only been isolated from the reaction of [$NiCl_2(PBu_3)_2$] with $Li_3P_7 \cdot 3\,DME$. The product formed has the composition [{Ni(PBu_3)$_2$}$_4$$P_{14}$] (**2**) [Eq. (b)]. In **2** the P_7 nortricyclane framework does not remain intact, but

$$[NiCl_2(PBu_3)_2] + Li_3P_7 \cdot 3\,DME \longrightarrow \underset{\mathbf{2}}{[\{Ni(PBu_3)_2\}_4P_{14}]} \qquad (b)$$

a P_{14} cage is formed that contains two linked P_7 units with norbornane-like structure (Fig. 2). The molecule has a crystallographic center of inversion between P7 and P7′. In the P_{14} cage three P atoms (P1, P4, P7) are bound to three other P atoms, whereas P2, P3, P5, and P6 are bound to two P atoms. According to the Zintl–Klemm concept, the extended Grimm–Sommerfeld rule, and the (8 − *n*) rule of Mooser and Pearson, the P atoms P1, P4, and P7 carry no charge, and P2, P3, P5, and P6 have one negative charge each.[14, 15] The [Ni(PBu_3)$_2$] fragments are bound to the P_2^{2-} pairs (P5–P6, P2–P3, and symmetry equivalent positions). In this assignment Ni is in the oxidation state +II, and **2** can therefore be described as [{Ni(PBu_3)$_2$}$^{2+}$]$_4$$P_{14}^{8-}$.

An alternative description of the bonding arrangement in **2** is the following: All P–P distances (220.2–224.1(4) pm) are in the expected range of P–P single bonds, with the exception of the P2–P3 (212.7(4) pm) and P5–P6 (213.1(4) pm) bonds, which are much shorter.[16] Therefore the P_{14} cluster could be better

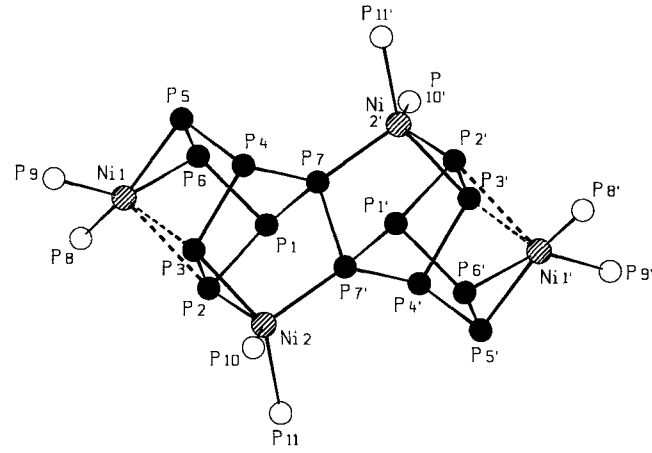

Fig. 2. Molecular structure of **2** (without Bu groups). Selected distances [±0.4 pm] and angles [±0.2°]: P1–P2 222.2, P1–P6 221.7, P1–P7 220.2, P2–P3 212.7, P3–P4 222.4, P4–P5 222.1, P4–P7 221.1, P5–P6 213.1, P7–P7′ 224.1, Ni1–P5 230.8, Ni1–P6 230.1, Ni1–P8 219.7, Ni1–P9 220.4, Ni1–P2 279.8, Ni1–P3 281.3, Ni2–P2 232.4, Ni2–P3 231.7, Ni2–P7 226.4, Ni2–P10 222.2, Ni2–P11 223.4, P6-P1-P2 96.2, P1-P2-P3 105.6, P2-P3-P4 106.0, P3-P4-P5 95.0, P4-P5-P6 105.3, P5-P6-P1 106.2, P1-P7-P4 98.3, P1-P7-P7′ 94.6, P9-Ni1-P6 143.6, P8-Ni1-P6 93.5, P7′-Ni2-P3 98.2, P10-Ni2-P7′ 110.3.

described as two linked P_7 cages with norbornadiene-like structure, where P2–P3 and P5–P6 are double bonds. These double bonds act as 2e donors for the uncharged [Ni(PBu_3)$_2$] fragments. The electronic structure calculations (vide infra) clearly favor the second alternative. Two PBu_3 groups (Ni1–P8 219.7(3); Ni1–P9 220.4(3) pm) and the double bond pairs P5–P6 (Ni1–P5 230.8(3); Ni1–P6 230.1(3) pm), and P2–P3 (Ni1–P2 279.8(3); Ni1–P3 281.3(3) pm) coordinate to Ni1 in a distorted tetrahedral fashion. The interaction of Ni1 with P2 and P3 is very weak as indicated by the long Ni–P distances, with Ni1 40 pm above the least-square mean plane of P5, P6, P8, and P9. Ni2 is also distorted tetrahedrally coordinated by the double bond P2–P3, P7′, P10, and P11 (Ni2–P2 232.4(3); Ni2–P3 231.7(3); Ni2–P7′ 226.4(3); Ni2–P10 222.2(3); Ni2–P11 223.4(3) pm). Assuming that the PBu_3 groups and the P–P double bonds are 2e donors, Ni1 has 16 and Ni2 18 valence electrons.

The ^{31}P NMR spectrum (Fig. 3) of **2**, which is almost temperature independent in the range of −80 to 50 °C, shows that the structure of the P_{14} cage in solution is about the same as in the solid state. A homoscalar correlated 2D $^{31}P\{^1H\}$ NMR spectrum (COSY90, THF/C_6D_6, 293 K) was employed to assign the signals at δ = 100.6 to the atoms P1 and P4. The resonance signals at δ = 127.6 and 9.8 belong to P7 and the P atoms of the PBu_3

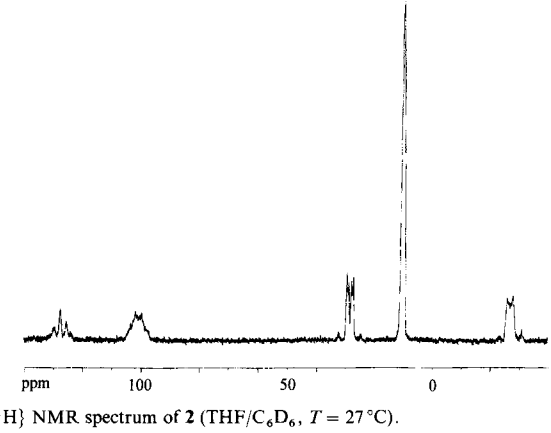

Fig. 3. $^{31}P\{^1H\}$ NMR spectrum of **2** (THF/C_6D_6, T = 27 °C).

groups, respectively. The multiplets at $\delta = 28.2$ and -27.0 can be assigned to P2,P3 and P5,P6 respectively. Obviously, in solution P2 and P3, P5 and P6 as well as P1 and P4 are equivalent. In the solid state a mirror plane through P7 and the Ni atoms is broken merely by the different orientation of the Bu groups of the PBu_3 ligands.

Reaction of in situ generated $[Cp^*CoCl]_2$ with $P_7(SiMe_3)_3$ gave a mixture of various products in low yields. So far, the only product to be structurally characterized is $[(Cp^*Co)_3P_6]$ (**3**) [Eq. (c)]. The analogous As compound has already been de-

$$[Cp^*CoCl]_2 + P_7(SiMe_3)_3 \longrightarrow \underset{\mathbf{3}}{[(Cp^*Co)_3P_6]} \quad (c)$$

scribed by Scherer et al.[17] In **3** (Fig. 4) three Cp*Co fragments are bridged by three P_2 units. Two P_2 units act as μ_3, η^2 bridges and one as a μ_2, η^2 bridge. The bond lengths P3–P4 and P5–P6 are 217.2(4) pm, typical for double bonds coordinating to metal atoms.[16] There might possibly be weak interactions between P3 and P6 (255.4(4) pm) and P4 and P5 (252.3(4) pm). The bond P1–P2 (204.7(4) pm) is unusually short. If the P_2 units are considered as 4e donors, all Co atoms achieve an 18 electron configuration. Obviously, the formation of **3** is the result of an unpredictable redox reaction in which the P_7 cage is destroyed.

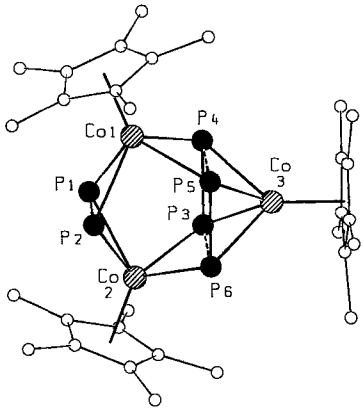

Fig. 4. Molecular structure of **3**. Selected distances [±0.4 pm] and angles [±0.4°]: P1–P2 204.7, P3–P4 217.1, P5–P6 217.2, P4···P5 252.3, P3···P6 255.4, Co1–P1 230.2, Co1–P2 230.6, Co1–P4 227.1, Co1–P5 226.6, Co2–P1 230.9, Co2–P2 230.5, Co2–P3 226.4, Co2–P6 226.7, Co3–P3 227.0, Co3–P4 228.6, Co3–P5 228.5, Co3–P6 227.9, P1-Co1-P2 52.7, P4-Co1-P5 67.6, P1-Co1-P4 79.9, P1-Co1-P5 109.1, P4-P3-P6 89.8, P3-Co3-P4 56.9, P3-Co3-P5 94.1, P3-Co3-P6 68.3.

This behavior was also observed in the reaction of $FeCl_2$ with LiCp* and $P_7(SiMe_3)_3$. A brown solution was formed at $-78\,^\circ C$ in THF. Layering this solution with heptane gave black crystals of **4** [Eq. (d)], which consists of $[(Cp^*Fe)_3P_6]^+$

$$FeCl_2 + LiCp^* + P_7(SiMe_3)_3 \xrightarrow{-78\,^\circ C} \underset{\mathbf{4}}{[(Cp^*Fe)_3P_6][FeCl_3(thf)]} \quad (d)$$

cations (Fig. 5) and $[FeCl_3(thf)]^-$ anions. To describe the bonding in terms of localized bonds is problematic, since the P–P distances vary from 226.8(1) to 249.8(2) pm. For this reason, a simple assignment of bonds is not possible. However, according to the Wade rules[18] the cation of **4** has 20 valence electrons for the cluster of six phosphorus and three iron atoms. This corresponds to the bonding structure found in $B_9H_9^{2-}$.[19] The distances in the polyhedra of the cation of **4** vary in a similar manner to those in $B_9H_9^{2-}$ (B–B 168–193 pm). The shortest P–P edge of the polyhedron is 226.8 pm (P1–P2), the longest 249.8(2) pm (P3–P3′). The Fe–P distances vary from 223.8(1) to 234.3(1) pm. A metal–metal bond between Fe1 and Fe2 is proposed because they are separated by 277.2(1) pm. An alternative description of **4** is that the P atoms form a distorted P_6 prismane with one P–P bond broken. The square planes coordinate to the Fe atoms of the Cp*Fe groups.

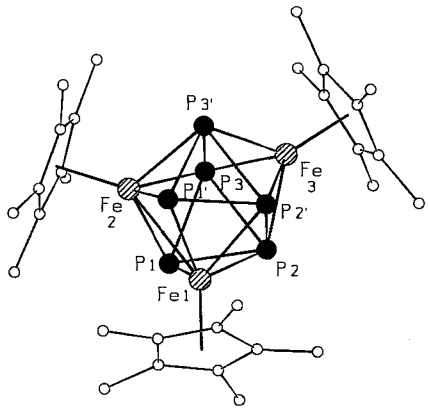

Fig. 5. Molecular structure of the $[(Cp^*Fe)_3P_6]^+$ cation in **4**. Selected distances [±0.5 pm] and angles [±0.5°]. For a better understanding of the cluster geometry P–P distances up to 250 pm were drawn as lines. P1–P2 226.8, P2–P3 239.3, P1–P3 227.2, P1···P1′ 411, P2–P2′ 248.2, P3–P3′ 249.8, Fe1–P1 225.5, Fe1–P2 234.3, Fe2–P1 225.5, Fe2–P3 234.3, Fe3–P2 224.4, Fe3–P3 223.8, Fe1–Fe2 277.2, P2-P1-P3 63.6, P1-P2-P3 58.3, P1-P3-P2 58.1, P1-P2-P2′ 103.6, P2-P3-P3′ 89.8, Fe2-Fe1-P2 85.1, Fe2-Fe1-P1 52.1, P3-Fe1-P3′ 67.9, P3-Fe3-P2 64.6, Fe2-P3-Fe3 106.4.

Reaction of the same starting compounds in THF at room temperature led to black crystals of **5** [Eq. (e)] after one day

$$FeCl_2 + LiCp^* + P_7(SiMe_3)_3 \xrightarrow{RT} \underset{\mathbf{5}}{[(Cp^*Fe)_3\{(\eta^3\text{-}P_3)Fe\}P_6]} \quad (e)$$

Figure 6 shows that the polyhedron consists of four iron and six phosphorus atoms. The Fe atoms Fe1, Fe2, and Fe2′ are coordinated by Cp* ligands, while Fe3 is coordinated by an

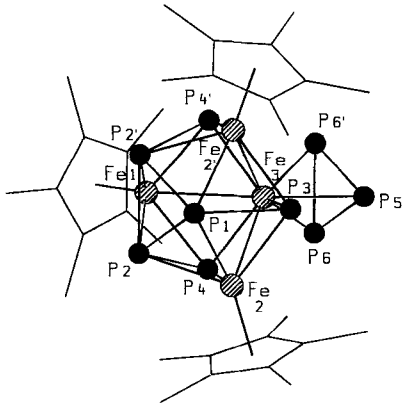

Fig. 6. Molecular structure of **5**. Selected distances [±0.2 pm] and angles [±0.1°]: Fe1–P2 229.7, Fe1–P4 226.9, Fe1–Fe3 274.9, Fe2–P1 230.2, Fe2–P2 229.9, Fe2–P3 227.0, Fe2–P4 226.9, Fe2–Fe3 274.9, Fe3–P3 217.9, Fe3–P4 217.9, Fe3–P5 233.1, Fe3–P6 233.8, P1–P2 233.0, P1–P3 241.3, P2–P2′ 232.6, P2–P4 241.4, P5–P6 210.7, P6–P6′ 211.7, P4-Fe1-P2 63.8, P4′-Fe1-P2 109.8, P2′-P2-P4 104.0, Fe1-Fe3-Fe2 83.0, P6-P5-P6′ 60.3.

η^3-P_3 ligand. The P_7 nortricyclane frame of the $P_7(SiMe_3)_3$ is still recognizable. The basal triangle is formed by P1, P2, and P2′ (P1–P2 233.0(1); P2–P2′ 232.6(2) pm); the equatorial positions are occupied by P3, P4, and P4′ (P1–P3 241.3(2); P2–P4 241.4(1) pm). The apical P atom is substituted by the (η^3-P_3)Fe group (Fe3–P5 233.1(2); Fe3–P6 233.8(1); P5–P6 210.7(2); P6–P6′ 211.7(2) pm). The three lateral faces of the nortricyclane framework are capped by Cp*Fe groups. These three Fe atoms bind to the apical Fe atom, Fe3, at a distance of

0947-6539/96/0202-0240 $ 10.00+.25/0 Chem. Eur. J. 1996, 2, No. 2

274.9(1) pm. In the polyhedron Fe3 has six neighbors, whereas in the corresponding boron hydride $B_{10}H_{10}^{2-}$ each B atom is bound to four or five other B atoms.[20] According to the Wade rules **5** is expected to have, analogous to $B_{10}H_{10}^{2-}$, 22 electrons for the bonds in the polyhedra. On condition that the *cyclo*-P_3 ligand is a 3e donor, **5** has only 20 electrons. The As homologue crystallizes with a similar structure and was described by Scherer et al.[21]

The product of the reaction of potassium and arsenic (K: As = 3:7, in liquid NH_3) with $[CoCl_2(PEt_2Ph)_2]$ in THF [Eq. (f)]

$$[CoCl_2(PEt_2Ph)_2] + \text{“}K_3As_7\text{”} \longrightarrow \underset{\mathbf{6}}{[Co_6As_{12}(PEt_2Ph)_6]} \quad (f)$$

has a very unusual structure. The product **6** (Fig. 7) consists of a heteroicosahedron formed by six Co atoms and six As atoms,

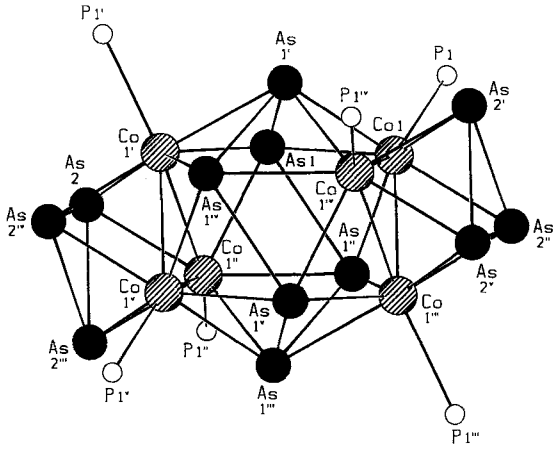

Fig. 7. Molecular structure of **6**. Selected distances [±0.4 pm] and angles [°]: As1–Co1′ 242.6, As1–Co1 250.5, As2–Co″ 233.6, As2–Co1′ 234.0, Co1–P1 221.2, Co1–Co1‴ 260.0, As1–As1′ 256.7, As2–As2‴ 254.1, As1′-As1-As1″ 104.0(1), Co1′-As1-Co1 106.7(1), Co1-As1-As1′ 57.2(1), As2′ᵛ-As2-Co1′ 57.02(9), Co1′-As2-As2‴ 90.78(8).

fused with two Co_3As_3 octahedra via the two Co_3 faces. In the heteroicosahedron, there is an As_6 ring in chair conformation with two Co_3 triangles completing the structure. Each Co atom is bound to three As atoms of the As_6 ring, two As atoms of the As_3 rings, and in addition to two Co atoms and the P atom of the PEt_2Ph ligands. As_3 rings like those in **6** have been observed in the cluster $[Co_4(\mu_3\text{-}As)_3(\mu_3,\eta^3\text{-}As_3)(PPh_3)_4]$.[22] The As–As distances within the As_3 and As_6 rings are 254.5(6)–256.4(4) pm, about 10 pm longer than in the above-mentioned Co_4 cluster, in As_4, and in $(AsPh)_6$.[22, 23] However, the As–As bond lengths in $[As_7Cr(CO)_3]^{3-}$ are 235–246 pm.[9] Similar bond lengths are found in $[(Cp^*Nb)_2As_8]$ (235.5–253.0 pm) and $[(Cp^*Nb)_2\{As_8Cr(CO)_5\}]$ (236.0–254.6 pm)[10, 4], but these complexes contain *cyclo*-As_8 rings. All known complexes with As_6 rings (e.g., $[(Cp^*Mo)_2As_6]$) have planar As_6 rings,[5] but a corrugated P_6 ring is known in the compound $[(Cp^*Ti)_2P_6]$.[6]

Molecular electronic structure calculations: To investigate the electronic structure, density functional theory (DFT) calculations[24] were carried out. This method has proved useful in the treatment of transition metal compounds.[25] The calculations were performed with the program system TURBOMOLE[26] employing the “Becke–Perdew functional” (B–P).[27] The molecular structures were optimized on the basis of analytical gradients by means of a relaxation procedure.[28] Phosphane ligands were modeled by PH_3 to reduce computational effort. This simplification should have only a minor effect on bonding in the cages.

Cage bonding in **6**: For **6** D_{3d} molecular symmetry was assumed and a total of 13 states differing in molecular orbital (MO) occupation and total spin were considered. Basis sets of the SVP type (split valence plus polarization)[29] were used; larger basis sets such as TZVP (triple zeta valence plus polarization)[30] did not lead to significant changes in structure parameters. The lowest energy was obtained for a diamagnetic state ($S = 0$) with the occupancy $[Co_6(PH_3)_6As_{12}]$: $42a_{1g}\ 14a_{2g}\ 55e_g\ 15a_{1u}\ 42a_{2u}\ 55e_u\ (^1A_{1g})$. This state also leads to good agreement of computed and measured structure constants; the largest deviation is 6 pm in the Co–Co bond length. All other electronic states show markedly larger deviations.

For the discussion of bonding in the fused cages of **6** we have to consider 90 electrons from Co 3d and As 4p atomic orbitals (AOs), which occupy the 45 high-lying MOs. These cage MOs are energetically well separated from As 4s AOs and interact only weakly with PH_3. Clearly, 24 electrons have to be assigned to the σ bonds in As rings. Of the remaining 66 electrons, 60 occupy MOs that are Co 3d or have an appreciable 3d participation (vide infra), and six are left for further cage bonds. The corresponding three MOs (one of a_{1g} and two of a_{2u} symmetry) are formed by linear combinations of Co 4s AOs and the $4p_\perp$ AO of As ($4p_\perp$ denotes here the 4p AO that is orthogonal to the plane formed by neighboring As atoms and is not involved in σ bonding).

A discussion of bonding in the Co–As cages has to be based on the energetic ordering of the AOs involved: As, $\varepsilon(4p) = -0.215$ hartree; Co, $\varepsilon(3d) \approx -0.2$ hartree; $\varepsilon(4s) \approx -0.18$ hartree. The orbital energy $\varepsilon(4p)$ results from the DFT calculation on the isolated As atom. $\varepsilon(3d)$ is inferred from the orbital energies of the MOs $13a_{2g}$ and $14a_{2g}$ of **6**; these MOs have almost pure d character, since no other a_{2g} orbitals are available for interaction (the energetically closest orbitals belong to the e type MOs of isolated PH_3). The 3d energy is in between the values obtained in atomic Co DFT calculations for occupancies $3d^7 4s^2$ and $3d^8 4s$, and thus points to an occupation of about $3d^{7.5}$ for Co. The Co 4s energy has consequently been assumed to be the average of (4s) values of the two Co occupations in question. Support for the d occupation of Co inferred from orbital energies is provided by the results of a Mulliken population analysis,[31] which yields $3d^{7.7}4s^{0.8}4p^{1.0}$ for Co and $4s^{1.8}4p^{3.0}$ for As.

The similarity of AO energies is an important characteristic of **6**: the d shells of Co are just filled to an extent that allows optimal resonance; this results in partly pronounced 3d (and 4s) participation in cage MOs. The valence MOs of the Co–As cages are, as a consequence, highly delocalized and not easily interpreted, but the following somewhat simplified picture describes the most important features of the electronic structure: Appreciable contributions of Co 3d AOs to cage bonding are only expected from the two d functions oriented in the tangent plane of the cage, for example, d_{xy} and $d_{x^2-y^2}$ in an appropriate local coordinate system. The As atoms nearest to Co form a distorted square, for example, As1, As1′ᵛ, As2, and As2′ᵛ relative to Co1 (Fig. 7). The lobes of the $3d_{xy}$ function point to these As atoms; this leads to optimal overlap with the $4p_\perp$ AOs of As available for cage bonding ($d_{x^2-y^2}$ consequently leads to smallest overlap).

The six functions of $3d_{xy}$ type give rise to irreducible representations a_{2g}, a_{1u}, e_g, and e_u. The a_{2g} and a_{1u} combinations have

no partners to interact with and are doubly occupied (vide supra). The e_g and e_u functions interact strongly with the corresponding functions of the $4p_\perp$ AOs of the As_6 ring, and to a lesser extent with those of the As_3 rings (which are high-lying π^* MOs). The Co–As bonding effected by these delocalized MOs is depicted in the contour diagram shown in Figure 8 (top). All other d functions of Co (except $3d_{xy}$) show smaller interactions and occupations relatively close to 2.0. The $3d_{xy}$ contribution to MOs of type e_g and e_u leads to eight electrons involved in cage bonding.

The other cage MOs mentioned above—one of type a_{1g} and two of a_{2u} character—involve Co 4s contributions. For both Co rings there is a bonding 4s combination describing a three-center bond, which yields an a_{1g} and an a_{2u} orbital for the two Co rings. These Co orbitals interact with the 4p π MO of the isolated As_3 ring; this also results in a_{1g} and a_{2u} MOs. The contour diagram Figure 8 (middle) shows the corresponding a_{1g} MO; the As_3–Co_3 bonding is clearly visible, as is the 4p π character (indicated by the node in the As_3 plane). The lowest-lying As_6 MO of dominant $4p_\perp$ character has a_{2u} symmetry (since there is no occupied σ MO of this symmetry, which would destabilize it), which leads to the bonding $Co_3(4s)$ $As_6(4p)$ $Co_3(4s)$ MO displayed in Figure 8 (bottom).

The above considerations can be summarized in the following way, starting from $2As_3^{3+}$ and As_6^{6+} with all σ bond MOs occupied and Co^+ with d^8 occupation, that is, $3d_{xy}$ is unoccupied and available for cage MOs. The remaining 18 electrons occupy three cage MOs with Co 4s and As $4p_\perp$ participation (one of a_{1g} and two of a_{2u} symmetry; Fig. 8, middle and bottom), four MOs with strong $3d_{xy}$ and As $4p_\perp$ participation (one of symmetry e_g and e_u each; Fig. 8, top), and the two nonbonding $3d_{xy}$ MOs of symmetry a_{2g} and a_{1u}. In addition to this schematic representation there are clearly slight delocalizations of Co d electrons into higher MOs of $4p_\perp$ and also σ* character.

As a support for our interpretation we report the computed shared electron numbers (SEN),[32] which are a measure of covalent bonding: SEN (As2 As2$''$) = 0.84; SEN (As1 As1′) = 0.82; SEN (As2 Co1′) = 0.33; SEN (As1 Co1′) = 0.28; SEN (As1′ Co′) = 0.23; SEN (Co1′ Co1″) = 0.15. These values indicate relatively weak As–As σ bonds—in agreement with somewhat elongated bond lengths—and weak but non-negligible covalent Co–As and Co–Co contributions. In agreement with the delocalized character of cage MOs discussed above, the population analysis further indicates multicenter effects, for example, SEN (As2′ As2″ As2$''$) = 0.21; SEN (As2′ As2″ Co1) = 0.10.

It remains to compare the analysis of the electronic structure in **6** with common formal descriptions of bonding in transition metal complexes. The counting rules of Wade[18] would assign 30 electrons to cage bonding; this corresponds to 24 electrons in As–As σ bonds plus six electrons in the a_{1g} and a_{2u} MOs (discussed above) with Co 4s participation. The electrons in the e_g and e_u MOs with strong $3d_{xy}$ participation were then assigned to Co, formally leading to a $3d^{10}$ occupation. This yields an oversimplified or even misleading picture. It is more appropriate to add the eight electrons in these e_g and e_u MOs to those involved in cage bonding; this leads to a total of 38 electrons, which is in accord with the $(2N+2)$ rule for an 18-atom cage. The $(2N+2)$ rule has proved useful for polyhedral cages (e.g., $B_{12}R_{12}^{2-}$), but is less useful for fused cages since the HOMO–LUMO gap is less pronounced than for simple polyhedral cages (the presence of heteroatoms adds to this difficulty). With these precautions in mind **6** can be considered to represent a case of $(2N+2)$ cage bonding with active participation of 3d AOs of Co.

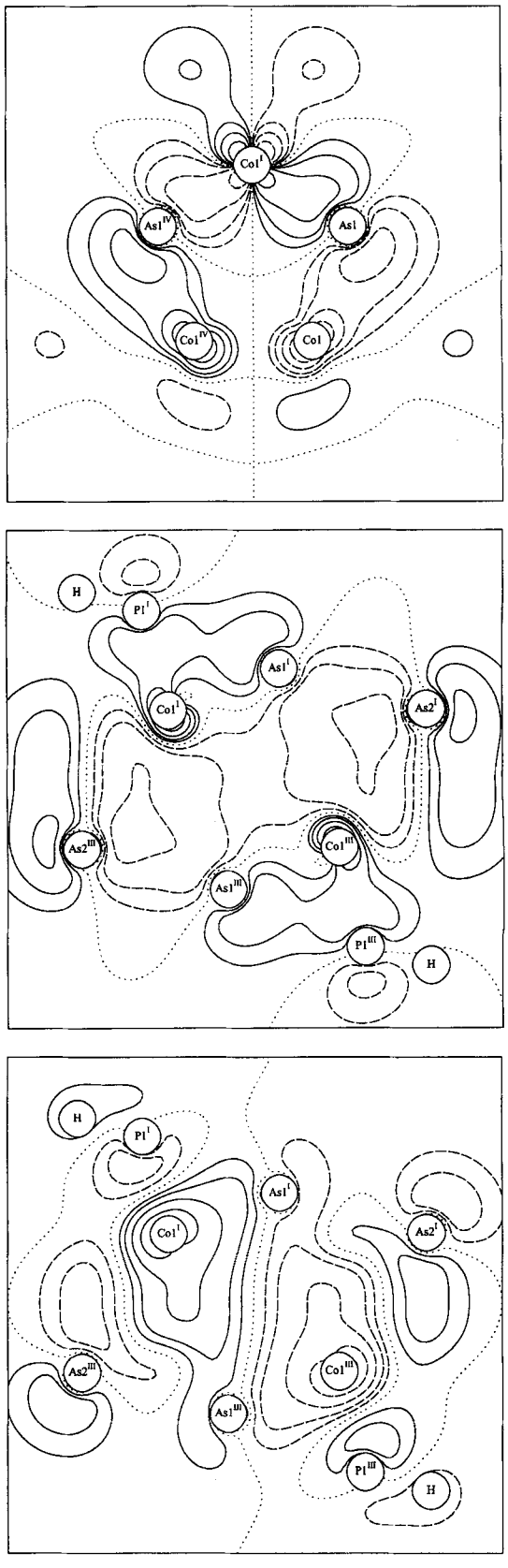

Fig. 8. MO contour diagrams that depict the bonding in the cage of **6**. Functional values: 0 (dotted), 0.001, 0.002, 0.004 etc. Top: section Co1 Co1′ Co1$''$; the e_u MO with bonding Co1′–As1 interaction, which is described by overlapping of Co $3d_{xz}$ and As 4p AO. Middle: section As1′ As2′ As2$'''$; the a_{1g} MO shows the bonding of the As_3 ring with the Co_3 rings through bonding linear combination of the As_3 π MO (indicated by the node in As2′) with the bonding Co_3 4s MO. Bottom: section As1′ As2′ As2$'''$; the a_{2u} MO describes, analogously to the middle diagram, the bonding of the Co_3 rings with the As_6 ring.

0947-6539/96/0202-0242 $ 10.00+.25/0 Chem. Eur. J. 1996, 2, No. 2

two possible interpretations (Klemm–Zintl concept with Ni^{II} versus π–π double bonds and Ni^0, as discussed above). C_{2h} symmetry was assumed, since this complies with structural data when the Bu groups are ignored. The DFT calculations have again been performed with the B–P[27] parametrization employing SVP[29] and TZVP[30] basis sets. The Bu groups were replaced by H.

The computed structure constants obtained with the smaller and larger basis sets differ, at most, by 4.4 pm in the bond lengths (Ni2–P7′, Fig. 2), but the larger basis gives consistently better agreement with experiment. The largest deviation in bond lengths between DFT/TZVP and experimental data reported above occurs for the Ni1-P2-P3 ring. The computed P2–P3 distance is 7 pm too long (all DFT methods give P–P distances that are 2 pm too long). The Ni1–P2 distance obtained is 258 pm (23 pm too short) but, even here, experiment and theory agree in giving a Ni–P distance that is much longer than found for typical Ni–P bonds (220 pm). The close agreement between measured and computed data is a strong indication that the correct occupation of molecular orbitals, which corresponds to a diamagnetic closed-shell case, has been selected by the program.

Population analyses[31, 32] first of all show that no major electron displacements take place: all Ni and P atoms are virtually neutral (absolute charges less than 0.3 for both basis sets). P2–P3 and P5–P6 show some double-bond character, but the π electron pairs are partly delocalized into Ni AOs. This is especially indicated by the SEN,[32] which are scattered around 1.07 for the single bonds and 1.33 for P2–P3 and P5–P6. The computed three-center SEN, such as SEN(Ni1 P5 P6) = 0.21, also conforms with the idea of delocalized π electron bond pairs.

Conclusion

Reactions of transition metal halogen complexes with Zintl anions of P and As open up an interesting new type of chemistry. In most cases the P_7 cage of the $Li_3P_7 \cdot 3DME$ or $P_7(SiMe_3)_3$ does not remain intact. In **2** a P_{14} framework is formed by two linked norbornadiene-like P_7 cages. In **3**, **4**, and **5** unpredictable redox reactions occur, and structures with P_2 fragments with double-bond character are observed. The Co–As cluster in **6** consists of a heteroicosahedron formed by six As and six Co atoms; in addition, two Co_3As_3 octahedra are linked to the heteroicosahedron by common Co_3 faces.

Density functional theory (DFT) calculations performed for **2** and **6** show good agreement of experimental and calculated structural data. The calculations confirm the norbornadiene-like bonding structure in **2** and a cage electron count of 38 for **6**.

Experimental Procedure

1: At −78 °C a solution of $[FeCp(CO)_2Br]$ (0.74 g, 2.88 mmol) in THF (15 mL) was slowly added to a solution of $Li_3P_7 \cdot 3DME$ (0.49 g, 0.96 mmol) in THF (50 mL). The dark red mixture was allowed to warm up to room temperature within 15 h. The solution was filtered and layered with 50 mL heptane. The product **1** could be obtained as crystalline red needles (30%, 0.23 g).

2: A solution of $[NiCl_2(PBu_3)_2]$ (2.12 g, 3.97 mmol) in THF (25 mL) was added to a solution of $Li_3P_7 \cdot 3DME$ (0.88 g, 1.73 mmol) in THF (25 mL) at room temperature. The solution immediately turned dark brown. The THF was removed in vacuo, the residue dissolved in heptane and filtered. Black crystals of **2** were obtained by slowly removing the solvent (13%, 0.26 g).

3: LiCp* (0.51 g, 3.59 mmol) and $CoCl_2$ (0.48 g, 3.70 mmol) were stirred at room temperature in THF (20 mL) for 15 min. The solvent was removed in vacuo, the residue dissolved in pentane and filtered. A solution of $P_7(SiMe_3)_3$ (0.51 g, 1.17 mmol) in toluene (5 mL) was added by diffusion. After one week a few crystals of **3** were isolated.

4, 5: $FeCl_2$ (0.56 g, 4.42 mmol) and LiCp* (0.59 g, 4.15 mmol) were suspended in THF (30 mL) at −78 °C. Addition of $P_7(SiMe_3)_3$ (0.63 g, 1.44 mmol) caused an immediate color change to dark brown. The mixture was allowed to warm up to room temperature within 15 h and was then filtered. Layering with heptane gave very air-sensitive brown crystals of **4** (11%, 0.18 g). MS (70 eV, EI, T = 270 °C): m/z (%): 759 (100) $[M^+]$, 624 (0.9) $[M^+ - Cp^*]$, 506 (7.7) $[M^+ - (Cp^*FeP_2)]$.
When the reaction was performed at room temperature, **5** crystallized as black crystals from the reaction solution after one day (26%, 0.28 g). MS (70 eV, EI, T = 300 °C): m/z (%): 908 (100) $[M^+]$, 759 (15.9) $[M^+ - (FeP^3)]$, 648 (3.8) $[M^+ - (Cp^*P_4)]$, 506 (3.9) $[M^+ - (Cp^*Fe_2P_5)]$.

6: $[CoCl_2(PEt_2Ph)_2]$ (0.56 g, 1.21 mmol) and 1.94 g of the product of the reaction of K with As (in liquid NH_3, ratio 3:7) were stirred in THF (50 mL) at room temperature. After a few minutes the solution turned dark brown. After one day half of the solvent was removed in vacuo. After 12 h black needles of **6** could be isolated (60%, 0.27 g)

X-Ray structure analysis: STOE IPDS imaging plate (**1–3, 6**) or STOE STADI IV (**4, 5**); $Mo_{K\alpha}$, T = −73 °C, data collection, structure solution (SHELXS-86) and refinement (SHELXL-93) of **1–6**:

1·THF: a = 1459.8(8), b = 2084(2), c = 2120(2) pm, V = 6451(8) × 10^6 pm^3; orthorhombic, *Pbca* (no. 61), Z = 8, $\mu(Mo_{K\alpha})$ = 1.72 mm^{-1}, $2\theta_{max}$ = 52°; 33527 reflections, 5963 independent reflections, 4027 [$I > 2\sigma(I)$] reflections observed, 364 parameters (Fe, P, C, O refined anisotropic, H calculated for idealized positions, one THF solvent molecule disordered); $R1$ = 0.056.

2: a = 1367.6(5), b = 1376.2(5), c = 1915.7(10) pm, α = 93.38(3), β = 109.53(3), γ = 108.16(3)°, V = 3175(2) × 10^6 pm^3; triclinic (no. 2), Z = 1, $\mu(Mo_{K\alpha})$ = 0.899 mm^{-1}, $2\theta_{max}$ = 52°; 22342 reflections, 11451 independent reflections, 8119 [$I > 2\sigma(I)$] reflections observed, 522 parameters (Ni, P, 37 C atoms of the Bu groups refined anisotropic, 9 C atoms refined isotropic, 4 of them disordered, H calculated for idealized positions for non disordered C atoms); $R1$ = 0.104.

3: a = 1157.9(3), b = 1486.7(6), c = 1969.9(5) pm, β = 99.73(2)°, V = 3342(2) × 10^6 pm^3; monoclinic, $P2_1/n$ (no. 14), Z = 4, $\mu(Mo_{K\alpha})$ = 1.779 mm^{-1}, $2\theta_{max}$ = 56°; 15563 reflections, 7603 independent reflections, 4021 [$I > 2\sigma(I)$] reflections observed, 363 parameters (Co, P, C refined anisotropic, Cp* group at Co3 disordered, H calculated for idealized positions); $R1$ = 0.088.

4: a = 1524.2(5), b = 3442.8(10), c = 1587.8(5) pm, V = 8332(5) × 10^6 pm^3; orthorhombic *Cmca* (no. 64), Z = 8, $\mu(Mo_{K\alpha})$ = 1.816 mm^{-1}, $2\theta_{max}$ = 56°; 7694 reflections, 5208 independent reflections, 3769 [$I > 2\sigma(I)$] reflections observed, 241 parameters (Fe, P, C of the cation refined anisotropic, H calculated for idealized positions, anion disordered); $R1$ = 0.040.

5·THF: a = 1592.7(4), b = 1730.6(6), c = 1452.7(4) pm, V = 4004(2) × 10^6 pm^3; orthorhombic, *Pnma* (no. 62), Z = 4, $\mu(Mo_{K\alpha})$ = 1.809 mm^{-1}, $2\theta_{max}$ = 54°; 5634 reflections, 4522 independent reflections, 3247 [$I > 2\sigma(I)$] reflections observed, 233 parameters (Fe, P, C refined anisotropic, H calculated for idealized positions, solvent molecule disordered); $R1$ = 0.031.

6: a = 2435.7(4), c = 1077.0(4) pm, V = 5533(2) × 10^6 pm^3; trigonal $R\bar{3}$ (no. 148), Z = 3, $\mu(Mo_{K\alpha})$ = 6.661 mm^{-1}, $2\theta_{max}$ = 50°; 6457 reflections, 2155 independent reflections, 1037 [$I > 2\sigma(I)$] reflections observed, 145 parameters (Co, As, P, C refined anisotropic, H calculated for idealized positions); $R1$ = 0.089. **6** also crystallizes with a different unit cell to **6**·3THF: a = 1763.9(3), c = 2444.3(5) pm, V = 6600(2) × 10^6 pm^3; trigonal $R\bar{3}$ (no. 148), Z = 3.

Acknowledgment: This work was supported by the Deutschen Forschungsgemeinschaft (SFB 195) and the Fonds der Chemischen Industrie.

Received: June 28, 1995 [F156]

[1] a) M. Baudler, *Angew. Chem.* **1987**, *99*, 429; *Angew. Chem. Int. Ed. Engl.* **1987**, *26*, 419; b) H. G. von Schnering, W. Hönle, *Chem. Rev.* **1988**, *88*, 243; c) H. G. von Schnering, *Angew. Chem.* **1981**, *93*, 44; *Angew. Chem. Int. Ed. Engl.* **1981**, *20*, 33; d) W. Hönle, H. G. von Schnering, *ibid.* **1986**, *98*, 370 and **1986**, *25*, 352.
[2] a) G. Fritz, H. W. Schneider, W. Hönle, H. G. von Schnering, *Z. Anorg. Allg. Chem.* **1990**, *584*, 21; **1990**, *585*, 51; b) G. Fritz, K. D. Hoppe, W. Hönle, D. Weber, D. Mujica, V. Manriquez, H. G. von Schnering, *J. Organomet. Chem.* **1983**, *249*, 63.
[3] M. Baudler, T. Etzbach, *Angew. Chem.* **1991**, *103*, 590; *Angew. Chem. Int. Ed. Engl.* **1991**, *30*, 580.

  0947-6539/96/0202-0243 $ 10.00+.25/0

[4] a) O. J. Scherer, *Angew. Chem.* **1990**, *102*, 1137; *Angew. Chem. Int. Ed. Engl.* **1990**, *29*, 1104; b) M. Scheer, E. Herrmann, *Z. Chem.* **1990**, *30*, 41; c) O. J. Scherer, T. Brück, *Angew. Chem.* **1987**, *99*, 59; *Angew. Chem. Int. Ed. Engl.* **1987**, *26*, 59; d) O. J. Scherer, H. Sitzmann, G. Wolmershäuser, *ibid.* **1985**, *97*, 358 and **1985**, *24*, 351; e) O. J. Scherer, R. Winter, G. Heckmann, G. Wolmershäuser, *ibid.* **1991**, *103*, 860 and **1991**, *30*, 850.

[5] a) G. L. Simon, L. F. Dahl, *J. Am. Chem. Soc.* **1973**, *95*, 2175; b) M. E. Barr, L. F. Dahl, *Organometallics* **1991**, *10*, 3991.

[6] O. J. Scherer, M. Swarowsky, G. Wolmershäuser, W. Kaim, S. Kohlmann, *Angew. Chem.* **1987**, *99*, 1178; *Angew. Chem. Int. Ed. Engl.* **1987**, *26*, 1153.

[7] S. Charles, B. W. Eichhorn, A. L. Rheingold, S. G. Bott, *J. Am. Chem. Soc.* **1994**, *116*, 8077.

[8] B. W. Eichhorn, R. C. Haushalter, J. C. Huffmann, *Angew. Chem.* **1989**, *101*, 1081; *Angew. Chem. Int. Ed. Engl.* **1989**, *28*, 1032.

[9] S. Charles, B. W. Eichhorn, S. G. Bott, *J. Am. Chem. Soc.* **1993**, *115*, 5837.

[10] H. G. von Schnering, J. Wolf, D. Weber, R. Ramirez, T. Meyer, *Angew. Chem.* **1986**, *98*, 372; *Angew. Chem. Int. Ed. Engl.* **1986**, *25*, 353.

[11] a) D. Fenske, J. Ohmer, J. Hachgenei, K. Merzweiler, *Angew. Chem.* **1988**, *100*, 1300; *Angew. Chem. Int. Ed. Engl.* **1988**, *27*, 1277; b) A. Eichhöfer, D. Fenske, W. Holstein, *ibid.* **1993**, *105*, 257 and **1993**, *32*, 242; c) H. Krautscheid, D. Fenske, G. Baum, M. Semmelmann, *ibid.* **1993**, *105*, 1364 and **1993**, *32*, 1302; d) D. Fenske, H. Krautscheid, *ibid.* **1990**, *102*, 1513 and **1990**, *29*, 1453; e) D. Fenske, J. Steck, *ibid.* **1993**, *105*, 254 and **1993**, *32*, 238; f) S. Dehnen, A. Schäfer, D. Fenske, R. Ahlrichs, *ibid.* **1994**, *106*, 786 and **1994**, *106*, 746; g) A. Eichhöfer, J. Eisenmann, D. Fenske, F. Simon, *Z. Anorg. Allg. Chem.* **1993**, *619*, 1360.

[12] For X-Ray structure analyses, see Experimental Procedure. Further details of the crystal structure investigations may be obtained from the Fachinformationszentrum Karlsruhe, D-76344 Eggenstein-Leopoldshafen (Germany), on quoting the depository numbers CSD-404523–404528.

[13] C. Mujica, D. Weber, H. G. von Schnering, *Z. Naturforsch.* **1986**, *41B*, 991.

[14] a) W. Klemm, *Proc. Chem. Soc. (London)* **1958**, 329; E. Zintl, *Angew. Chem.* **1939**, *52*, 1; b) H. G. von Schnering, *Angew. Chem.* **1981**, *93*, 44; *Angew. Chem. Int. Ed. Engl.* **1981**, *20*, 33.

[15] a) E. Mooser, W. B. Pearson, *Phys. Rev.* **1956**, *101*, 1608; b) H. O. Grimm, A. Sommerfeld, *Z. Phys.* **1926**, *36*, 36.

[16] G. Huttner, J. Borm, L. Zsolnai, *J. Organomet. Chem.* **1986**, *304*, 309.

[17] O. J. Scherer, K. Pfeiffer, G. Heckmann, G. Wolmershäuser, *J. Organomet. Chem.* **1992**, *425*, 141.

[18] K. Wade, *Adv. Inorg. Chem. Radiochem.* **1976**, *18*, 1.

[19] L. J. Guggenberger, *Inorg. Chem.* **1968**, *7*, 2260.

[20] R. D. Dobrott, W. N. Lipscomb, *J. Chem. Phys.* **1962**, *37*, 1779.

[21] O. J. Scherer, C. Blath, G. Heckmann, G. Wolmershäuser, *J. Organomet. Chem.* **1991**, *409*, C15.

[22] D. Fenske, J. Hachgenei, *Angew. Chem.* **1986**, *98*, 165; *Angew. Chem. Int. Ed. Engl.* **1986**, *25*, 175.

[23] U. Hedberg, E. W. Hughes, J. Wiezer, *Acta Cryst.* **1961**, *143*, 369.

[24] R. G. Parr, W. Yang, *Density-Functional Theory of Atoms and Molecules* (Oxford University, New York, 1989).

[25] T. Ziegler, *Chem. Rev.* **1991**, *91*, 651.

[26] a) R. Ahlrichs, M. Bär, M. Häser, H. Horn, C. Kölmel, *Chem. Phys. Lett.* **1989**, *162*, 165; b) O. Treutler, R. Ahlrichs, *J. Chem. Phys.* **1995**, *102*, 346.

[27] a) A. D. Becke, *Phys. Rev. B.* **1988**, *38*, 3098; b) S. H. Vosko, L. Wilk, M. Nusair, *Can. J. Phys.* **1980**, *58*, 1200; c) J. P. Perdew, *Phys. Rev. B* **1986**, *33*, 8822.

[28] Geometry optimization terminated after the total gradient norm was smaller than 10^{-3} for Cartesian coordinates (in atomic units) and for internal coordinates (atomic units and radians).

[29] A. Schäfer, H. Horn, R. Ahlrichs, *J. Chem. Phys.* **1992**, *97*, 2571.

[30] A. Schäfer, C. Huber, R. Ahlrichs, *J. Chem. Phys.* **1994**, *100*, 5829.

[31] R. S. Mulliken, *J. Phys. Chem.* **1950**, *72*, 4493.

[32] Population analysis based on occupation numbers, C. Erhardt, R. Ahlrichs, *Theor. Chim. Acta* **1985**, *68*, 231; a typical SEN value for As–As single bonds (As_4 molecule) is 1.0.

0947-6539/96/0202-0244 $ 10.00+.25/0